Proposal of a Colombian Refrigeration Potential Map Based on Solar Powered Absorption Cooling Systems

Jhojan Stiven Zea Fernández [iD]**, Mario Luna-delRisco** [iD]**,**
Valeria Berrocal [iD]**, Nildia Yamileth Mejias Brizuela,**
Carlos Arrieta González [iD]**, Laura Paniagua** [iD]**,**
Sebastian Villegas Moncada [iD]**, and Carlos A. Arredondo Orozco** [iD]

1 Introduction

The growing concern about the effects of global warming, as well as the uncertainty due to finite reserves of fossil fuels, have turned the world's attention to nonconventional renewable energy sources as the way to a clean and environmentally friendly energy transition [2]. Colombia has pledged to take part in this transition through international agreements such as the Paris agreement [3]; however, the country is still lagging in the development of renewable energy sources in the national territory.

By 2021, less than 1% of the electricity generated in the country comes from nonrenewable energy sources such as biomass, solar, and wind energy, a very low percentage compared to more developed countries such as the United States, where 12% of the energy consumed comes from these sources [4]. According to the accelerated growth of renewable energy for the next decade, Colombia has set itself the goal of reaching 15% share of renewables by 2030, with emphasis on the north coast of the country [5], where there is great potential for solar and wind energy [6].

In view of the accelerated growth expected for renewable energy in the next decade, emphasis must be placed on how these new technologies can help

J. S. Zea Fernández · M. Luna-delRisco (✉) · V. Berrocal · C. Arrieta González
S. Villegas Moncada · C. A. Arredondo Orozco
Universidad de Medellín, Medellín, Colombia
e-mail: mluna@udemedellin.edu.co

N. Y. Mejias Brizuela
Universidad Politécnica de Sinaloa, Mazatlán, México

L. Paniagua
Benemerita Universidad Autónoma de Puebla, Puebla, México

low-income people with no access to electrical energy. In Colombia, approximately 52% of the national territory is not connected to the electrical grid; this means that almost 2 million people who live in these places get sporadic and low-quality access to electricity or no access at all [1]. Since a large part of the people who live in non-interconnected areas engage in productive activities such as livestock, fishing, and agriculture, it is to be expected that part of the production is lost because they cannot cool their products.

The implementation of absorption cooling cycles that can use solar energy as a heat source means that large cooling centers could be available to residents of non-interconnected areas as a way of storing their products for later sale [7], thereby increasing the economic development and life quality [8]. However, not all areas of the country are suitable for the installation of these systems, since there are a wide variety of climates and weather conditions [9].

The objective of this chapter is to present a map of the absorption cooling potential for the Colombian territory. Maximum cooling volume capacity was determined based on data of solar radiation and temperature (mean values). Those variables were also used for the calculation of the system´s efficiency allowing the geolocation of non-interconnected areas where the industrial facilities might be placed.

2   System Description

The system consists of a condenser, an evaporator, an absorber, a generator, a pump, expansion valves, a heat exchanger, and a solar collector, as shown in Fig. 1.

The cycle is possible because of the ability of certain substances to perform absorption and desorption reactions. In this case, water absorbs ammonia vapor in the absorber and creates a solution with a weak water concentration; the solution has its pressure increased by means of a pump and is sent to the generator, in which the heat coming from the solar collector heats the solution and causes most of the ammonia vapor to be desorbed.

The high-pressure ammonia vapor shifts to liquid phase in the condenser and is expanded to a low pressure with an expansion valve; the low-pressure liquid is then converted into ammonia vapor in the evaporator and is sent to the absorber to restart the cycle. The solution that is left on the generator, now with a strong water concentration, exchanges heat with the refrigerant flow exiting the pump to increase the system's efficiency and is expanded, using an expansion valve to go once again into the absorber [10].

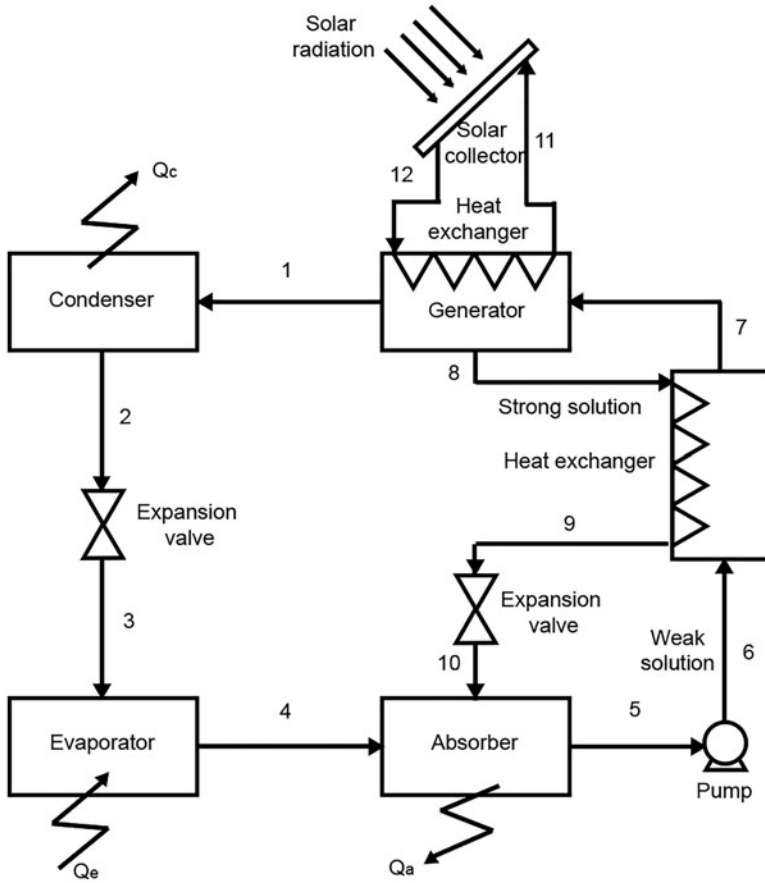**Fig. 1** System schematic

3 Modeling and Methodology

3.1 Symbols and Subscripts

Symbols

COP
    = Coefficient of performance
E   = Efficiency
f   = Mass flow ratio
h   = Enthalpy [kJ/kg]
P   = Pressure [kPa]
$\dot{m}$ = Mass flow [kg/s]

q   = Heat per unit mass [kJ/kg]
Q   = Heat [kJ]
Q   = Heat rate [kW]
T   = Temperature [°C]
⬚ = Power [kW]
x   = Concentration [kg/kg]
G_{stc}
    = Global irradiance on standard test conditions [1000 W/m^2]

    Subscripts

a   = Absorber
b   = Pump
c   = Condenser
e   = Evaporator
l   = Liquid
g   = Generator
sc = Solar collector
ref = Refrigerant
sf = Strong solution
sd = Weak solution
v   = Vapor

3.2   Thermodynamic Model

A simple steady-state model was considered for this particular study. There was no
need for a thermal energy storage system. The model assumes heat and pressure
losses on all the piping and units to be negligible and the refrigerant to be 100%
ammonia (NH$_3$) [11]. The mass balances are presented in Eqs. 1, 2, 3, 4, 5, 6, 7, 8, 9,
10 and 11 [11]:

$$\dot{m}_1 = \dot{m}_2 \tag{1}$$

$$\dot{m}_2 = \dot{m}_3 = \dot{m}_{ref} \tag{2}$$

$$\dot{m}_3 = \dot{m}_4 = \dot{m}_{ref} \tag{3}$$

$$\dot{m}_4 + \dot{m}_{10} = \dot{m}_5 \tag{4}$$

$$\dot{m}_9 = \dot{m}_{10} \tag{5}$$

$$\dot{m}_5 = \dot{m}_6 \tag{6}$$

$$\dot{m}_7 = \dot{m}_1 + \dot{m}_8 \tag{7}$$

$$\dot{m}_8 + \dot{m}_6 = \dot{m}_7 + \dot{m}_9 \tag{8}$$

$$\dot{m}_4 + \dot{m}_{10} = \dot{m}_5 \tag{9}$$

$$\dot{m}_9 = \dot{m}_8 \tag{10}$$

$$\dot{m}_{11} = \dot{m}_{12} \tag{11}$$

The generator is possible to perform an NH_3 balance, as seen in Eq. 12 [11]:

$$\dot{m}_7 x_7 = \dot{m}_1 x_1 + \dot{m}_8 x_8 \tag{12}$$

Equations 13 and 14, which are expressions for the strong solution mass flow rates, can be obtained from Eqs. 12 and 7 [11]:

$$\dot{m}_8 = \frac{x_7 - x_1}{x_8 - x_7} \dot{m}_1 \tag{13}$$

$$\dot{m}_7 = \frac{x_8 - x_1}{x_8 - x_7} \dot{m}_1 \tag{14}$$

From Eq. 13, the circulation ratio can be formulated as [11]:

$$f = \frac{\dot{m}_7}{\dot{m}_1} = \frac{x_8 - x_1}{x_8 - x_7} \tag{15}$$

The energy balances are performed as follows in Eqs. 16, 17, 18, 19, 20, 21, 22, 23, 24 and 25 [11]:

$$\dot{Q}_c = \dot{m}_{ref}(h_1 - h_2) \tag{16}$$

$$h_2 = h_3 \tag{17}$$

$$\dot{Q}_e = \dot{m}_{ref}(h_4 - h_3) \tag{18}$$

$$\dot{Q}_a = \dot{m}_4 h_4 + \dot{m}_{10} h_{10} - \dot{m}_5 h_5 \tag{19}$$

$$\dot{W}_b = \dot{m}_5(h_6 - h_5) \tag{20}$$

$$h_7 = h_6 + \frac{\dot{m}_8}{\dot{m}_6}(h_8 - h_9) \tag{21}$$

$$h_9 = h_{10} \tag{22}$$

$$\dot{m}_{12}(h_{12} - h_{11}) = \dot{m}_1 h_1 + \dot{m}_8 h_8 - \dot{m}_7 h_7 \tag{23}$$

$$\dot{m}_{12}(h_{12} - h_{11}) = G_{stc} A_{sc} E_{sc} \tag{24}$$

$$COP = \left[\frac{\dot{Q}_e}{G_{stc} A_{sc} E_{sc} + \dot{W}_b} \right] \tag{25}$$

The authors express Eq. 18 in terms of the circulation ratio when dividing the whole expression by $\dot{m}_4$ as presented in Eq. 26 [11]:

$$q_a = (h_5 - h_{10}) + f(h_{10} - h_5) \tag{26}$$

3.3   Methodology

The previous equations present an ideal absorption cooling system with no thermal energy storage system, assuming reference conditions for variables such as pressures and temperatures [12]. The model calculates the heat extracted by the heat pump ($\dot{Q}_e$) based on the solar irradiance and ambient temperature of a particular location.

A MATLAB script identifies the color of each pixel on the average ambient temperature and average peak sun hours (PSH) maps that the Institute of Hydrology, Meteorology and Environmental Studies (IDEAM) provides [13] [14] and translates it into usable data. The script then calculates the amount of daily cooling each pixel of the map can generate and the efficiency of the system (expressed by the COP on each pixel).

The thermodynamic properties for the NH_3-H_2O mixture are calculated with the equations proposed by Sun [15]. Then, in each pixel, the system is simulated by setting Tc to the mean ambient temperature of each pixel. In this simulation, the solar collector receives a constant solar irradiance of 1000 W/m^2. The cycle works for the equivalent time to PSH of the pixel by calculating the daily amount of cooling and the system efficiency depending on the ambient temperature.

The result is a map of the country in which each pixel has a value for maximum amount of cooling produced with 1 m^2 of solar collector and the system's efficiency, detailing the potential for the solar absorption system in every location of the region. The reference conditions considered were as follows:

T_g = 80 °C
T_a = 25 °C
T_e = -5 °C
$\dot{m}$ = 1 kg/s
E_{sc} = 90%
A_{sc} = 1 m^2

4   Results

The generated maps for daily cooling potential and system efficiency are presented in Figs. 2 and 3.
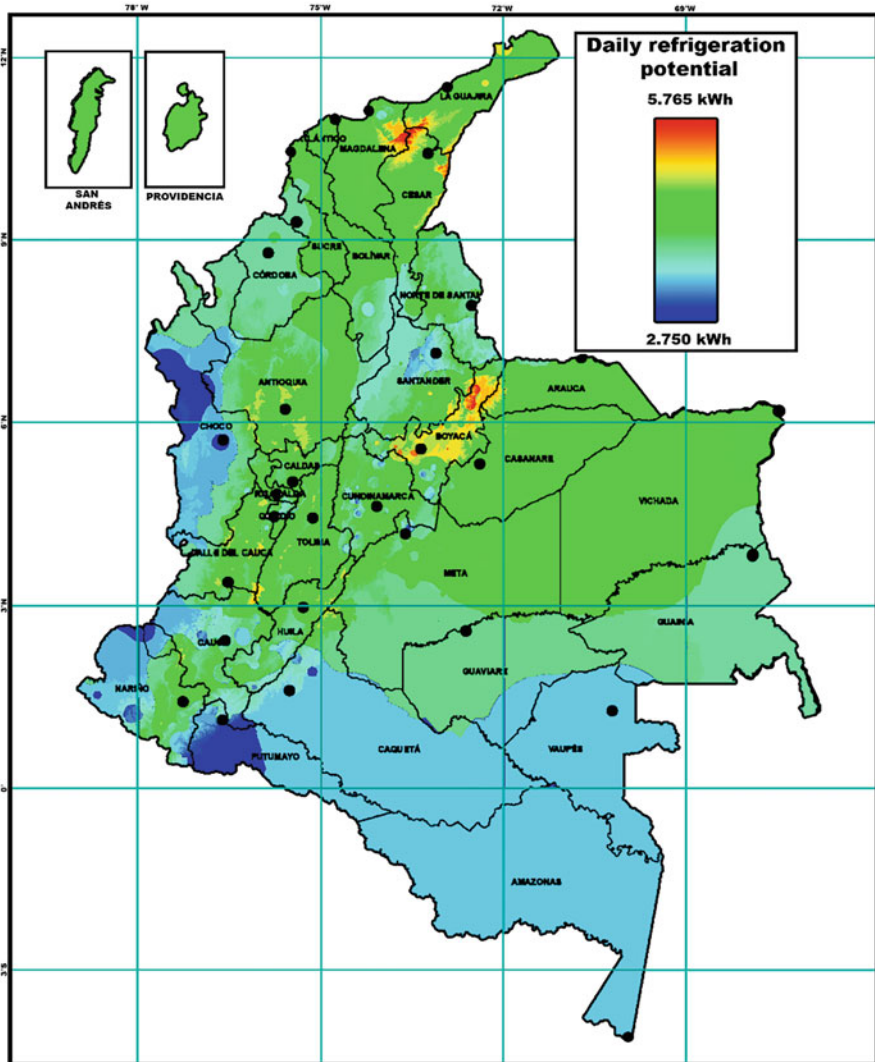
Fig. 2 Daily refrigeration potential map

5 Discussion

Since Colombia is a tropical country, there are no significant climatic variabilities due to the lack of seasons. Temperature conditions in any given location depend highly on the altitude. With this in mind, it can be determined that Fig. 3, which presents the system's efficiency, follows the contour of the relief in the national territory. There are higher COPs (1.10–1.22) in places such as the Andes Mountain

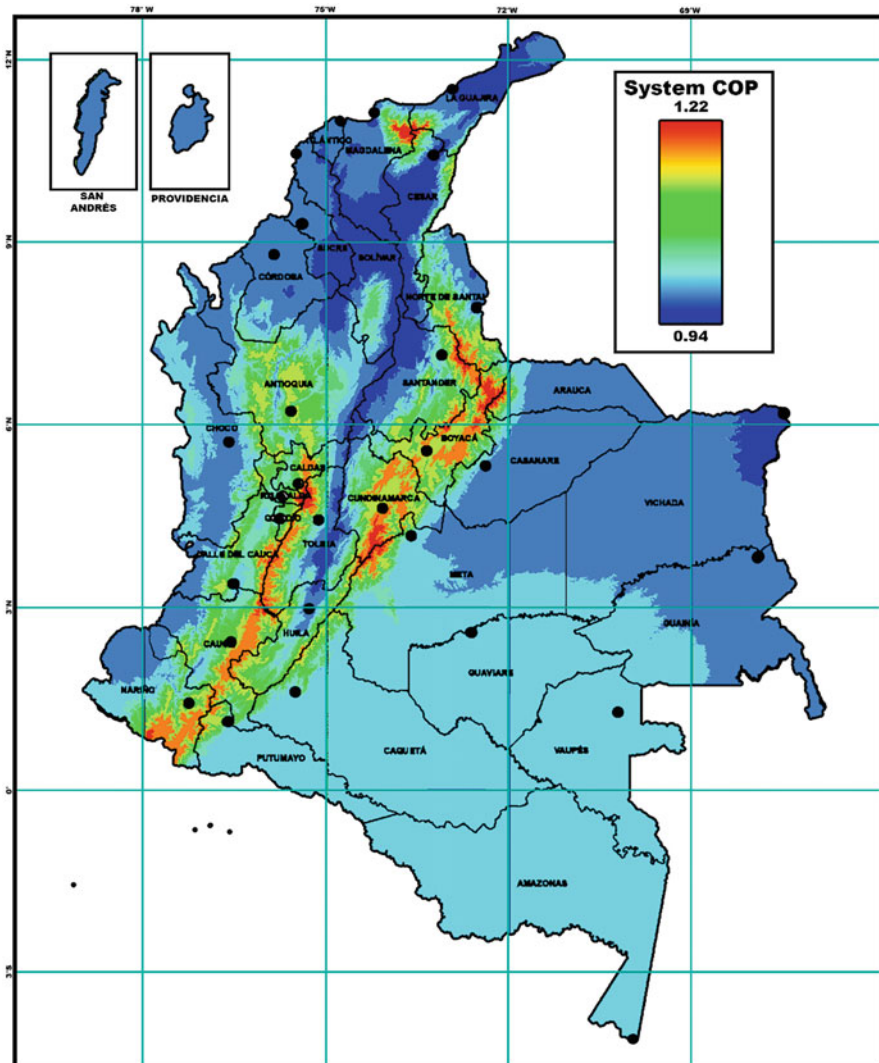**Fig. 3** System COP map

range or the snowy Sierra of Santa Marta. Moderate COPs (1–1.12) are in the Amazon area of the country, the high plains, and the pacific coast, whereas low performances (COP= 0.94–1) are in the Atlantic coast and the High Guajira.

The highest amount of cooling potential (5.4–5.765 kWh) was found in areas with low temperatures and high irradiations, such as the high mountains of Boyacá and the snowy Sierra of Santa Marta. All three branches of the Andes Mountain range across the country present high refrigeration potential (5.0–5.5 kWh) because of the low temperatures. The East Plains, the Atlantic Coast, and the San Andres and

Providencia Islands offer good potentials despite high temperatures (4.25–5.1 kWh). This phenomenon can be explained because these regions are the ones with the highest irradiation in the country.

The departments of Cordoba, Guainía, and Guaviare present moderate cooling potentials (3.5–4.33 kWh) because of high temperatures and low irradiation. The Pacific Coast and Amazon regions of the country are the ones that offer the lowest potentials (2.750–3.45 kWh). This can be explained because of the hot temperatures and low irradiances due to the high levels of cloudiness and rainfall that characterize these regions.

The northern part of the Guajira and the insular regions are the non-interconnected zones that would be the most attractive for the implementation of solar powered absorption cooling systems because of high potentials and the economic activities in which the lifestyle in these regions is based. The locals live mostly from fishing, livestock, and tourism [1], and the electricity is generated from fossil fuels. Fuel supply for this territory is inconsistent and unreliable. Construction of massive cooling systems that are solar powered can improve the quality of life of the inhabitants of these places by offering them a way to store their products and cool their hotels and inns without relying on fossil fuels. Additionally, this technology also offers a high potential for mitigating CO_2 emissions.

As for the Amazon and Pacific Coast, the other two identified non-interconnected regions presented a low potential for these cooling systems.

The results of this research are limited by a number of factors such as the use of multi-annual average ambient temperature and solar radiation, the lack of consideration of energy losses due to the non-ideality of real systems, and the steady nature of the equations used.

6　Conclusions

The outcome maps of this study suggest that solar powered absorption systems are a good and viable method for cooling generation in non-interconnected areas of Colombia such as the High Guajira, San Andres, and Providencia Islands, where locals live mainly from fishing, livestock, and tourism. This system will lead to an increase of the quality of life without CO_2 emissions. The Pacific Coast and Amazon region of the country present the lowest potential of any non-interconnected zone in Colombia. In these places, the implementation of these systems would be more costly because of the increased area of solar collection that is needed to meet the demands of the inhabitants.

This map uses multi-annual average radiation and temperature data, and because of the equatorial location of the country, the climate can change significantly from one day to the other in any given place, and this means that the system efficiency and performance can be diminished or enhanced due to the environmental conditions, but even if the maps do not exactly predict the daily behavior of the system, they are a good tool to estimate the mean amount of refrigeration a system can produce on

any part of the country. Also it can be used to calculate the solar collection area needed to achieve a certain amount of cooling power since the maps are based on a 1 m^2 solar collector.

Future studies that can be done to further increase the understanding of the applicability of solar powered absorption systems on the Colombian territory include a transient simulation for the operation of the system on a whole day, with real data from minute-to-minute measurements rather than average solar radiation and ambient temperature. Additionally, including entropy and exergy analyses to the energy and mass balances to account for losses and the irreversibility of the system will make the results more exact and useful.

References

1. Superintendencia de Industria y Comercio, "ZONAS NO INTERCONECTADAS - ZNI Diagnóstico de la prestación del servicio de energía eléctrica 2017 Superintendencia Delegada para Energía y Gas Combustible," no. 1, p. 74, 2017.
2. Gielen, D., Boshell, F., Saygin, D., Bazilian, M. D., Wagner, N., & Gorini, R. (2019). The role of renewable energy in the global energy transformation. *Energy Strategy Reviews, 24-*(January), 38–50.
3. Ministerio de Ambiente. (2009) *El Acuerdo de Paris, asía actuará Colombia frente al Cambio Climático*.
4. U. E. I. Administration, "Energy outlook 2021," vol. 2021, no. January, pp. 1–22, 2021.
5. UPME, "Plan Energético Nacional 2021–2051," p. 2015, 2021.
6. Ojeda, C. E., Candelo, B. J. E., & Silva, O. J. I. (2017). Caracterización de los potenciales de Energía Solar y Eólica para la integración de Proyectos sostenibles en Comunidades Indígenas en La Guajira Colombia. *Espacios, 38*(37), 11.
7. Al-Hamed, K. H. M., & Dincer, I. (2019). Investigation of a concentrated solar-geothermal integrated system with a combined ejector-absorption refrigeration cycle for a small community. *International Journal of Refrigeration, 106*, 407–426.
8. Aguilar-Jiménez, J. A., et al. (2020). Optimum operational strategies for a solar absorption cooling system in an isolated school of Mexico. *International Journal of Refrigeration, 112*, 1–13.
9. IDEAM. (2018). Carácterísticas Climatológicas De Ciudades Principales Y Municipios Turísticos. *Inst. Hidrol. Meteorol. y Estud. Ambient.*, 48.
10. Nikbakhti, R., Wang, X., Hussein, A. K., & Iranmanesh, A. (2020). Absorption cooling systems – Review of various techniques for energy performance enhancement. *Alexandria Engineering Journal, 59*(2), 707–738.
11. A. J. Bula, D. L. Herrera, L. F. Navarro, and L. A Corredor, "Thermodynamic Simulation of a Solar Absorption Refrigeration System Generator – Heat Exchanger," *AMSE* no. 2000, 2000.
12. Wang, J., Qi, X., Ren, F., Zhang, G., & Wang, J. (2021). Optimal design of hybrid combined cooling, heating and power systems considering the uncertainties of load demands and renewable energy sources. *Journal of Cleaner Production, 281*, 125357.
13. IDEAM. (2014). "Distribución de la temperatura media anual (°C). Promedio multianual 1981–2010.," p. 1.
14. Francisco, A. R. L. (2013). Atlas climatológico, radiación y viento en Colombia. *Journal of Chemical Information and Modeling, 53*(9), 1689–1699.
15. Taylor, P., Sun, D., & Sun, D. (2007). Computer simulation and optimization of ammonia-water absorption refrigeration systems. *Energy Sources, 2013*, 37–41.